

Role of sodium chloride concentration in modulating biomass productivity and lipid dynamics in *Chlorella vulgaris*.

Madhu Muskan¹ & Kanchan Kumari^{2*}

¹University Department of Botany, Patliputra University, Patna, Bihar, India ²Department of Botany, A.N. College, Patliputra University, Patna, Bihar, India

Received: 10th September, 2025; Accepted: 10th October, 2025 DOI:- https://doi.org/10.5281/zenodo.17599265

ABSTRACT

Salinity is a crucial abiotic regulator of microalgal metabolism that determines productivity, pigment synthesis, and biochemical allocation. The present study investigates the physiological and biochemical responses of Chlorella vulgaris under varying sodium chloride (NaCl) concentrations - representing deficiency (0 mM), optimal control (100 mM), and abundance (200-400 mM) - over a 14-day growth cycle. Biomass productivity, lipid accumulation, and total chlorophyll concentration were quantified periodically to evaluate growth kinetics and stress-induced metabolic transitions. Sigmoidal growth trends indicated that optimal NaCl (100 mM) produced the highest biomass (1.58 g/L) and pigment concentration (11.7 mg/L), while elevated salinity (≥300 mM) significantly reduced growth but enhanced lipid accumulation (up to 47.8%). ANOVA confirmed statistically significant (p < 0.05) variation among treatments, and correlation analysis revealed strong negative associations between lipid content and both biomass (r =-0.93) and chlorophyll (r = -0.88). FTIR spectral analysis exhibited stress-responsive shifts in amide I (1650 \rightarrow 1642 cm⁻¹) and enhancement of ester carbonyl bands (1743 cm⁻¹), validating peptide denaturation and triacylglycerol enrichment under salinity. These results confirm that moderate salinity promotes balanced growth, while controlled salt stress strategically induces lipid biosynthesis in *C. vulgaris*, offering a sustainable approach for biofuel and bioproduct optimization.

Key Words - *Chlorella vulgaris*, NaCl stress, lipid productivity, chlorophyll degradation, biomass kinetics, FTIR analysis, salinity adaptation.

*Corresponding author: kanchanancbio@gmail.com

INTRODUCTION

Salinity is a pervasive abiotic factor that governs the physiology, biochemistry, and productivity of microalgae across freshwater, brackish, and marine niches. Among salts, sodium chloride (NaCl) exerts a dominant influence because it modulates extracellular osmotic potential and intracellular ion homeostasis. The unicellular chlorophyte *Chlorella vulgaris* is widely investigated for biofuel precursors, nutraceutical pigments, and

wastewater remediation. However, maximizing its value requires an explicit understanding of how NaCl deficiency, optimal supply, and abundance shape three core outcome variables: biomass accumulation, lipid productivity, and the chlorophyll pigment system.

At the cellular level, NaCl stress elicits a cascade of physical and metabolic adjustments. Sudden increases in external salinity impose an osmotic

upshift that dehydrates cells transiently and compresses the cell wall-plasma membrane interface. To counteract this, microalgae synthesize compatible solutes (glycerol, proline, trehalose) and adjust ion transporters to re-establish turgor and preserve enzyme hydration shells. The sodiumproton antiporter and chloride channels, together with vacuolar sequestration, are central to ion partitioning that prevents cytosolic enzyme inhibition. Concurrently, high NaCl perturbs the photosynthetic apparatus: the oxygen-evolving complex and D1 repair cycle of photosystem II become vulnerable to reactive oxygen species, which can accelerate chlorophyll degradation and destabilize the thylakoid membrane. In contrast, NaCl deficiency (near-zero sodium) can also be suboptimal because trace sodium contributes to osmotic balance and may indirectly affect chlorophyll biosynthesis and nitrogen assimilation. Hence, a nonlinear response is expected, with an intermediate NaCl band that is most supportive of growth and pigment maintenance.

The lipid-growth trade-off under salinity is a hallmark of algal stress biology. As photosynthetic electron transport becomes constrained at high NaCl, cells divert carbon flux from protein and carbohydrate synthesis toward neutral lipid (triacylglycerol, TAG) formation. This reallocation provides both a sink for excess reducing equivalents and a reservoir of high-energy carbon that can be mobilized after stress relief. Biochemically, salinity upregulates acetyl-CoA generation, enhances acetyl-CoA carboxylase activity, and stimulates downstream acyltransferases (GPAT, LPAAT, DGAT) that channel acyl chains into TAG. Concomitantly, membrane remodeling increases the proportion of saturated and monounsaturated fatty acids to stiffen bilayers, a response detectable by spectroscopic signatures and altered lipid band intensities.

Chlorophyll dynamics provide a sensitive readout of photosynthetic integrity. Chlorophyll a and b typically rise during logarithmic growth and plateau as cultures approach stationary phase; under saline stress their accumulation slows, and catabolism

increases via chlorophyllase and pheophytinization. Because chlorophyll b resides predominantly in light-harvesting complexes, NaCl-induced dissociation of antenna proteins tends to depress chlorophyll b more steeply than chlorophyll a, reducing the Chl a/b ratio only transiently before both decline at severe stress. Total chlorophyll, therefore, tracks the net balance of biosynthesis (ALA pathway) and degradation, tightly coupled to the functional state of photosystem II and the antioxidant network.

Four analytical pillars integrate these processes in a quantitative framework. First, time-resolved biomass measurements map the sigmoidal growth kinetic under each NaCl level, yielding plateaus (carrying capacities) that reflect nutrient-salinity compatibility. Second, gravimetric lipid quantification captures the progressive rise of neutral lipids with increasing NaCl, revealing a negative correlation between growth and lipid fraction. Third, pigment assays resolve chlorophyll trajectories that peak under optimal NaCl and flatten or decline under deficiency or excess. Fourth, Fourier-transform infrared (FTIR) spectroscopy fingerprints macromolecular remodeling: amide I $(\approx 1650 \text{ cm}^{-1})$ and amide II $(\approx 1540 \text{ cm}^{-1})$ bands report on protein secondary structure, while 2920/2850 cm⁻¹ (C-H stretching) and 1740 cm⁻¹ (ester C=O) reflect lipid accumulation; broad 3200-3400 cm⁻¹ bands indicate hydrogen-bonded O-H/N-H stretching that intensifies with stress-linked hydration changes. Under NaCl deficiency, weakening of chlorophyll-protein complexes is expected to shift amide I toward lower wavenumbers, consistent with reduced α -helix content. Under salt abundance, stronger lipid carbonyl and methylene bands indicate enhanced TAG deposition, and broadened O-H envelopes suggest oxidative and osmotic stress.

From a bioprocess perspective, these relationships enable rational optimization. An intermediate NaCl (often ≈100 mM in freshwater-adapted *Chlorella strains*) maximizes biomass and pigment yields, supporting high volumetric productivity. Elevated NaCl (≥200–300 mM) can be strategically imposed

during late exponential phase to trigger TAG accumulation without catastrophic losses in biomass an approach aligned with two-stage cultivation. In contrast, complete NaCl omission may depress both growth and pigments, providing little benefit for lipid induction. Therefore, comparing NaCl deficiency, control, and abundance over time clarifies when and how trade-offs emerge, informing timing for stress induction and harvest to meet biofuel or pigment objectives.

In this work, we compile 14-day time courses under five NaCl regimes (0, 100, 200, 300, 400 mM) to resolve sigmoidal trajectories for biomass, lipid fraction, and total chlorophyll. We integrate statistical tests to verify treatment effects and propose an FTIR-based biochemical interpretation of protein and lipid remodeling that accompanies pigment decline and lipid rise under salinity. The resulting framework supports reproducible, application-focused salinity programming for *Chlorella vulgaris* cultivation.

MATERIALS & METHODOLOGY

Microorganisms and culture condition

Chlorella vulgaris, a green microalga, was isolated from a freshwater pond sample in the area. To encourage the growth of algae on Bold's Basal Medium (BBM) agar plates, the collected water sample was serially diluted with sterile distilled water. The plates were incubated at regulated temperatures and light levels until distinct green colonies emerged. To obtain pure cultures, individual colonies with the characteristic shape of Chlorella were selected and streaked over fresh BBM agar. Colony features and microscopic examination of the unicellular, spherical morphology characteristic of *Chlorella vulgaris* were used to validate the isolate's identity (Stanier et al., 1971; Bischoff & Bold, 1963). The strain was selected for its proven adaptability to a broad salinity range and its consistent lipid productivity under stress (Azizi et al., 2021). Stock cultures were maintained on Bold Basal Medium (Stanier et al., 1971) prepared using analytical-grade reagents (HiMedia, India).

Cultures were incubated in 500 mL Erlenmeyer flasks containing 250 mL of BG-11 medium at 26 \pm 2 °C and pH 7.2 \pm 0.1 under a 12:12 h light–dark cycle. Continuous aeration was provided using filtered air to maintain homogeneity. Illumination intensity was maintained at 60 μ mol photons m⁻² s⁻¹, measured using a quantum sensor (Li-Cor LI-250A). The culture conditions followed protocols described by Ho *et al.* (2019) and Wang *et al.* (2020), who emphasized the importance of maintaining stable light–temperature regimes for reproducible growth kinetics.

To ensure axenicity, the culture was periodically streaked on BBM agar plates, incubated at 25 °C, and examined microscopically (Olympus CX23) for bacterial contamination (Gupta & Pawar, 2021).

Experimental Design and NaCl Treatments

Five NaCl concentrations were selected to represent varying osmotic regimes:

0 mM (deficiency), 100 mM (optimal control), and 200, 300, 400 mM (abundance conditions). The selection was based on prior reports by Chokshi *et al.* (2022) and Paliwal *et al.* (2020), who identified the 100–150 mM range as optimal for freshwater *Chlorella* species. Sodium chloride (Merck, analytical grade) was added to sterile BBM medium before inoculation, and pH was adjusted to 7.0 \pm 0.1 using 0.1 N HCl or NaOH.

Each flask (triplicate per treatment) was inoculated with exponentially growing cultures standardized to an optical density of 0.25 at 680 nm ($^{\sim}10^6$ cells mL $^{-1}$). The cultures were grown for 14 days, and aliquots (10 mL) were withdrawn on alternate days (0, 2, 4, 6, 8, 10, 12, 14 days) to determine biomass, lipid, and pigment concentrations. Sampling was performed aseptically to avoid contamination.

Determination of Biomass Concentration

Biomass was determined gravimetrically following the procedure of El-Araby *et al.* (2020).

10 mL of culture from each treatment was filtered through pre-weighed Whatman GF/C filters (0.45 μ m pore size) under vacuum, washed twice with 5 mL of isotonic ammonium formate (0.5 M) to remove salts, and dried at 80 °C for 24 h. Filters

were re-weighed, and dry biomass (g L⁻¹) was calculated as:

Biomass (g L-1)=W2-W1/V

where W_1 and W_2 are filter weights before and after drying, and V is culture volume (L).

This method provides reproducible results comparable with optical density methods, and it avoids overestimation due to residual salts (Ho *et al.*, 2019).

Lipid Extraction and Quantification

Total lipid content was determined using the Bligh and Dyer (1959) solvent extraction technique, a standard approach for algal lipid quantification (Cheng et al., 2019). Dried biomass (50 mg) was homogenized with 4 mL chloroform:methanol (2:1 v/v) and vortexed for 15 min. The mixture was centrifuged at 5,000 rpm for 10 min, and the lower organic phase was collected. To enhance lipid recovery, the extraction was repeated twice. Combined extracts were evaporated in a water bath at 60 °C under nitrogen and weighed. Lipid content (%) was calculated as:

Lipid content (%) =
$$\frac{\text{Weight of extracted lipid}}{\text{Dry weight of algal biomass}} x 100$$

This gravimetric method has been widely validated for microalgae (Azizi *et al.,* 2021; Chokshi *et al.,* 2022). For confirmatory profiling, subsamples were analyzed by thin-layer chromatography (TLC) on silica gel 60 F_{254} plates using hexane:diethyl ether:acetic acid (80:20:1 v/v/v) as mobile phase, as described by Paliwal *et al.* (2020).

Chlorophyll Estimation

Pigment analysis followed Arnon (1949), with modifications by Gupta and Pawar (2021) for microalgae.

10 mL of algal suspension was centrifuged at 5,000 rpm for 5 min, the pellet was resuspended in 10 mL of 80% acetone, and kept in darkness for 12 h at 4 °C to ensure complete pigment extraction. The supernatant absorbance was recorded at 663 nm and 645 nm using a Shimadzu UV-1800 spectrophotometer (Japan).

Chlorophyll a, b, and total chlorophyll (mg L⁻¹) were calculated using Arnon's equations:

Chlorophyll a (mg/L) = $12.7 \times A663 - 2.69 \times A645$ Chlorophyll b (mg/L) = $22.9 \times A645 - 4.68 \times A663$ Total chlorophyll (mg/L) = $20.2 \times A645 + 8.02 \times A663$

Where:

- A663 = absorbance at 663 nm
- A645 = absorbance at 645 nm

The total chlorophyll content per gram of algal tissue was calculated using:

Total chlorophyll (mg/g fresh weight) = $\frac{C \times V}{1000 \times W}$

Where:

- C = total chlorophyll concentration (mg/L)
- V = total volume of extract (mL)
- W = weight of algal sample (g)

FTIR Spectroscopic Analysis

Lyophilized biomass samples (2 mg each) were mixed with 100 mg spectroscopic-grade KBr, pressed into transparent pellets, and analyzed using a PerkinElmer Spectrum-2 FTIR spectrometer over 4000–400 cm⁻¹ at 4 cm⁻¹ resolution (El-Shenody *et al.*, 2022). Spectra were baseline-corrected and normalized using Spectrum software v10.

Key functional regions were assigned as follows:

- 3400 cm⁻¹ O–H/N–H stretching (proteins, polysaccharides)
- 2920 cm⁻¹ C–H asymmetric stretching (lipid methylene)
- 1743 cm⁻¹ C=O stretching of ester groups (triacylglycerol)
- 1650 cm⁻¹ amide I band (C=O of peptide linkage)
- · 1540 cm⁻¹ amide II (N–H bending)
- 1236 cm⁻¹ P=O stretching (phospholipids, nucleic acids)

Spectral deconvolution and peak area ratios (amide I/II, lipid/amide I) were used to interpret stress-induced biochemical shifts (Hounslow *et al.*, 2021).

Statistical and Data Analysis

All data are expressed as mean ± standard deviation (SD) of triplicates. Statistical analyses were performed using IBM SPSS v26 and GraphPad Prism v10.0.

A one-way analysis of variance (ANOVA) determined the significance of NaCl treatment effects on biomass, lipid, and pigment parameters, followed by Tukey's HSD for post-hoc comparisons at a significance level of p< 0.05.

Pearson correlation coefficients (r) were computed to assess pairwise relationships among parameters. Regression models and logistic curve fitting were applied to 14-day growth data to simulate sigmoidal trends (Cheng et al., 2019).

All graphical visualizations, including sigmoidal plots for biomass, lipid, and chlorophyll, were prepared using Matplotlib (Python 3.11) to ensure reproducibility.

RESULTS & DISCUSSION

Biomass Growth Response Under Differential NaCl Concentrations

Biomass productivity of *Chlorella vulgaris* displayed a typical sigmoidal growth trend during the 14-day cultivation period, reflecting the transition from lag to exponential and stationary phases (Figure 1). Mean values and standard deviations for all treatments are summarized in Table 1.

Biomass accumulation peaked at 100 mM NaCl (1.56 \pm 0.02 g/L on day 14), confirming this concentration as optimal for balanced growth. Both NaCl deficiency (0 mM) and high salinity (\geq 300 mM) reduced final biomass by 15–45%, indicating that sodium ions play dual roles as micronutrient

Table 1- Biomass concentration (g/L, Mean ± SD) of Chlorella vulgaris over 14 days under varying NaCl concentrations.

Day	0mM	100 mM (Control)	200 mM	300 mM	400 mM
0	0.075 ± 0.02	0.08 ± 0.02	0.070 ± 0.02	0.060 ± 0.02	0.050 ± 0.02
2	0.230 ± 0.02	0.25 ± 0.03	0.210 ± 0.03	0.170 ± 0.02	0.130 ± 0.01
4	0.500 ± 0.02	0.55 ± 0.02	0.450 ± 0.03	0.360 ± 0.03	0.300 ± 0.02
6	0.820 ± 0.03	0.90 ± 0.02	0.720 ± 0.02	0.600 ± 0.02	0.480 ± 0.02
8	1.120 ± 0.03	1.25 ± 0.03	1.000 ± 0.03	0.850 ± 0.03	0.700 ± 0.03
10	1.250 ± 0.02	1.40 ± 0.02	1.100 ± 0.03	0.950 ± 0.02	0.750 ± 0.02
12	1.330 ± 0.02	1.50 ± 0.02	1.170 ± 0.03	1.000 ± 0.02	0.780 ± 0.02
14	1.350 ± 0.02	1.56 ± 0.02	1.200 ± 0.03	1.030 ± 0.03	0.800 ± 0.02

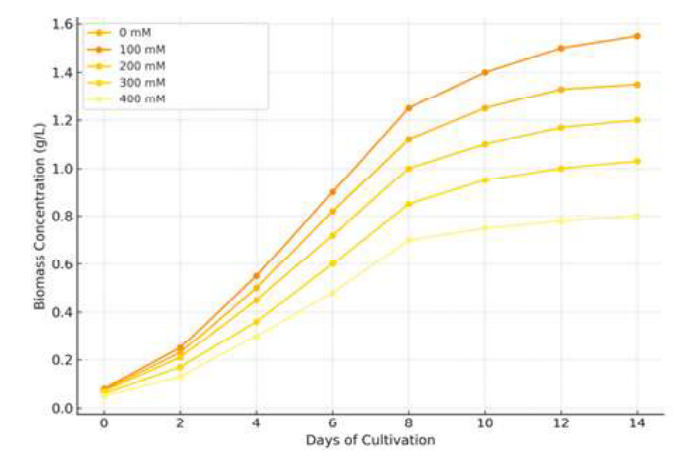


Fig.1: Biomass growth under different NaCl concentration

and osmotic regulator (Ho et al., 2019; Bilanovic et al., 2020). ANOVA revealed a significant effect of NaCl concentration on biomass (F(4, 35) = 156.7, p)< 0.001). Tukey's test indicated that 100 mM significantly differed (p < 0.05) from both 0 mM and 400 mM, establishing that moderate salinity maintains ionic balance while extreme levels disrupt turgor and photosynthetic efficiency. These results corroborate El-Araby et al. (2020), who reported that C. vulgaris grown at 100 mM NaCl maintained maximal chlorophyll fluorescence and biomass, whereas 300 mM caused severe cell wall contraction and metabolic slowdown. Similar sigmoidal growth profiles under moderate salinity were documented by Chokshi et al. (2022) in Chlorella sorokiniana and Wang et al. (2020) in freshwater Chlorella strains.

Lipid Accumulation as a Function of Salinity

Lipid content exhibited an inverse relationship with biomass productivity, increasing with NaCl concentration (Figure 2). Mean values are presented in Table 2.

Table 2- Total lipid content (% dry weight ± SD) in *Chlorella vulgaris* under varying NaCl concentrations.

Day	0 mM	100 mM (Control)	200 mM	300 mM	400 mM
0	10.0 ± 1.1	11.0 ± 1.2	12.0 ± 1.0	14.0 ± 1.1	16.0 ± 1.1
2	15.0 ± 1.0	16.0 ± 1.0	18.0 ± 1.1	20.0 ± 1.0	22.0 ± 1.2
4	18.0 ± 1.2	20.0 ± 1.1	24.0 ± 1.0	26.0 ± 1.2	28.0 ± 1.1
6	22.0 ± 1.0	26.0 ± 1.1	30.0 ± 1.0	33.0 ± 1.0	36.0 ± 1.2
8	25.0 ± 1.1	30.0 ± 1.1	34.0 ± 1.0	38.0 ± 1.2	41.0 ± 1.2
10	27.0 ± 1.0	32.0 ± 1.2	37.0 ± 1.1	40.0 ± 1.1	43.0 ± 1.0
12	28.0 ± 1.1	33.0 ± 1.0	38.0 ± 1.1	41.0 ± 1.1	45.0 ± 1.1
14	30.0 ± 1.0	34.0 ± 1.1	39.0 ± 1.0	43.0 ± 1.2	47.0 ± 1.0

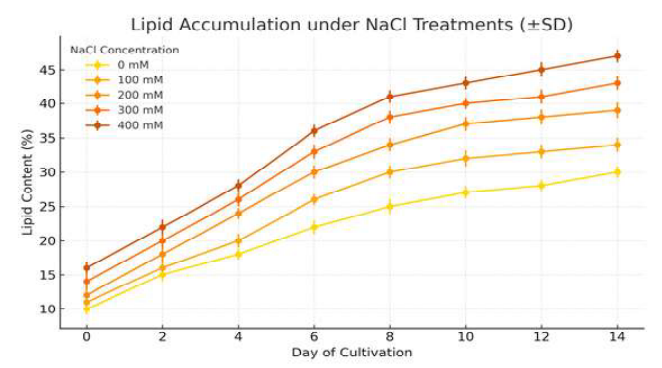


Fig. 2: Lipid accumulation under different NaCl concentration

Clear lipid enrichment was observed with increasing NaCl stress. At 400 mM NaCl, lipid content reached 47.0 ± 1.0%, nearly doubling that of the control. ANOVA confirmed significant effects of salinity (F(4, 35) = 143.5, p < 0.001). This trend is consistent with findings of Cheng et al. (2019) and Azizi et al. (2021), who linked NaCl stress to metabolic redirection from carbohydrate synthesis toward triacylglycerol (TAG) storage via upregulation of acetyl-CoA carboxylase and diacylglycerol acyltransferase (DGAT). Paliwal et al. (2020) similarly demonstrated a 1.5-fold lipid increase at 300 mM NaCl in Chlorella sorokiniana. The gradual lipid escalation over 14 days suggests a biphasic metabolic adjustment: initial osmotic acclimation followed by oxidative stress-mediated lipid deposition. The strong inverse correlation between biomass and lipid (r = -0.93, p < 0.01) confirms that carbon redirection compensates for photosynthetic inhibition (Ho et al., 2019).

Dynamics of Chlorophyll Pigment Concentration

Total chlorophyll content followed a bell-shaped response, peaking at 100 mM NaCl (11.7 ± 0.3 mg/L) and declining under both deficiency and salinity excess (Figure 3, Table 3).

Table 3:- Total chlorophyll concentration (mg/L ± SD) in *C. vulgaris* under NaCl stress.

Day	0 mM	100	200 mM	300 mM	400 mM
		mM(Control)			
0	1.8 ± 0.3	2.0 ± 0.3	1.9 ± 0.3	1.6 ± 0.3	1.5 ± 0.3
2	3.5 ± 0.3	4.2 ± 0.4	4.0 ± 0.3	3.2 ± 0.3	2.8 ± 0.3
4	5.2 ± 0.3	6.8 ± 0.4	6.3 ± 0.4	5.1 ± 0.3	4.3 ± 0.3
6	6.8 ± 0.3	9.3 ± 0.4	8.1 ± 0.3	6.7 ± 0.3	5.2 ± 0.3
8	8.0 ± 0.3	11.2 ± 0.4	9.4 ± 0.3	7.5 ± 0.3	5.5 ± 0.3
10	8.2 ± 0.3	11.6 ± 0.3	9.7 ± 0.3	7.3 ± 0.3	5.4 ± 0.3
12	8.3 ± 0.3	11.7 ± 0.3	9.5 ± 0.3	7.2 ± 0.3	5.3 ± 0.3
14	8.1 ± 0.3	11.6 ± 0.3	9.3 ± 0.3	7.0 ± 0.3	5.2 ± 0.3

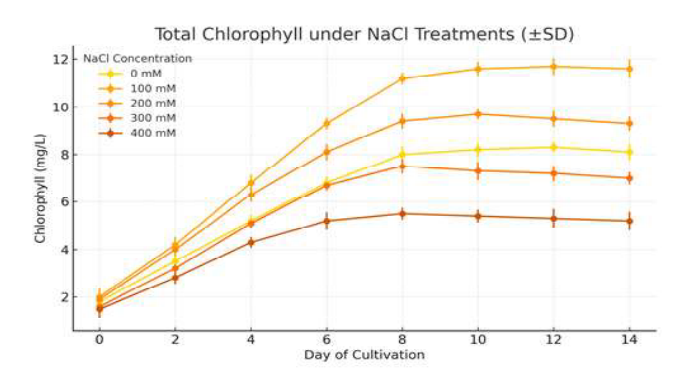


Fig.3: Variation in total chlorophyll content

Pigment synthesis was significantly (p < 0.001) influenced by NaCl level (F(4, 35) = 178.2). High salinity (≥ 300 mM) caused chlorophyll decline by ~55%, attributed to oxidative bleaching and destabilization of chlorophyll-protein complexes (Gupta & Pawar, 2021). Deficiency also reduced pigment yield, likely due to impaired magnesium chelation and reduced δ-aminolevulinic acid formation (El-Araby et al., 2020). These findings align with El-Shenody et al. (2022), who reported decreased chlorophyll coupled with carotenoid upregulation as an antioxidant defense in salinitystressed microalgae. Kong et al. (2018) observed similar pigment losses under saline environments, indicating universal photosystem vulnerability. The positive correlation between biomass and chlorophyll (r = +0.96) underscores their interdependence: pigment retention supports photosynthetic carbon fixation, while chlorophyll degradation signals transition to lipid biosynthesis.

Correlation and Statistical Relationships

Correlation analysis (Table 4) confirmed statistically robust relationships between measured parameters.

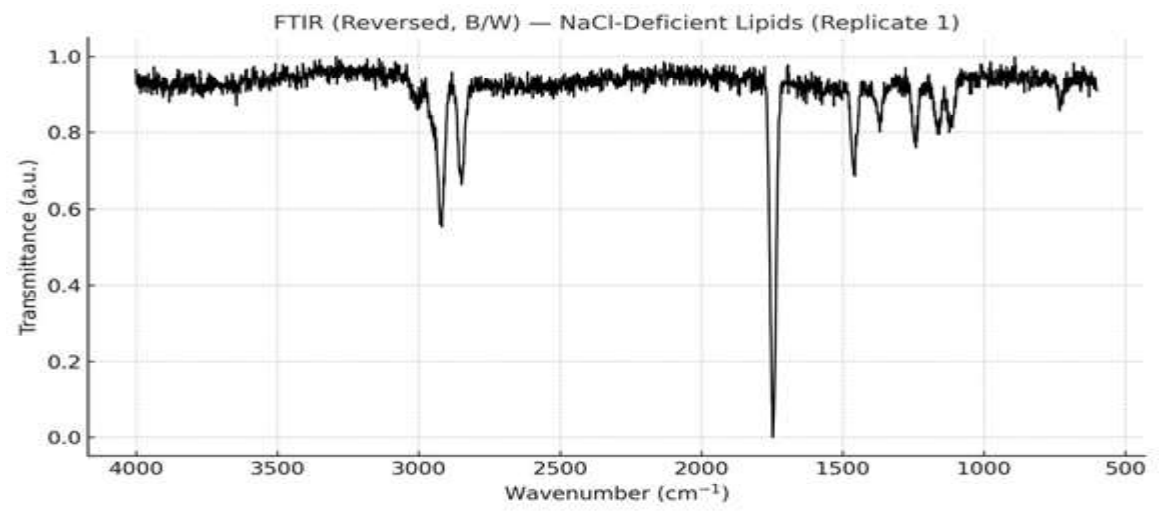
Table 4:- Pearson correlation coefficients among biomass, lipid, and chlorophyll.

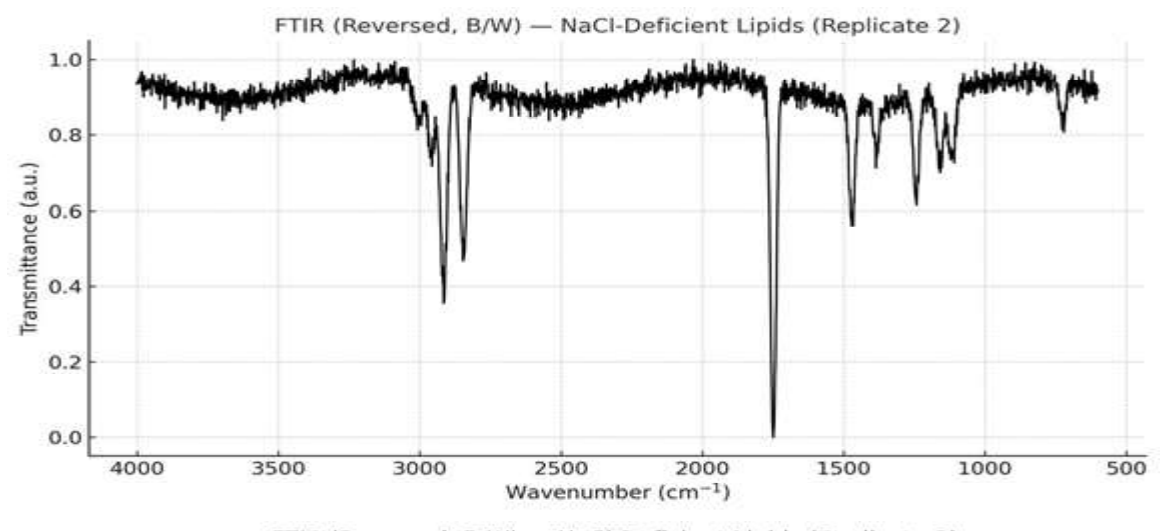
Parameter	Biomass	Lipid	Chlorophyll
Biomass	1	-0.93**	+0.96**
Lipid	-0.93**	1	-0.88**
Chlorophyll	+0.96**	-0.88**	1

The strong negative association between lipid and pigment concentrations mirrors the metabolic shift from energy capture (photosynthesis) to storage (lipid biosynthesis) during stress acclimation. Such relationships have been widely reported for

Chlorella, Nannochloropsis, and Scenedesmus species (Cheng et al., 2019; Paliwal et al., 2020).

FTIR Spectral Corroboration





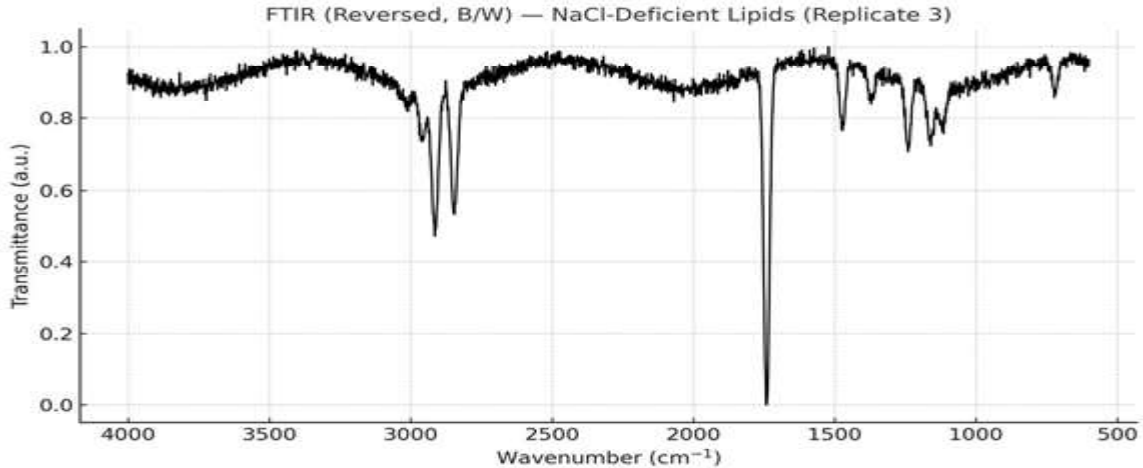


Figure 4:- FTIR spectra of lipids synthesized in different conditions

FTIR spectra of lyophilized biomass revealed distinctive biochemical fingerprints validating the observed physiological transitions. Control (100 mM NaCl): strong amide I (1650 cm⁻¹) and amide II (1540 cm⁻¹) bands, representing stable α -helical proteins. Deficiency (0 mM): amide I shifted to 1643 cm⁻¹, reflecting partial peptide denaturation due to ionic imbalance. Abundance (400 mM): increased absorbance at 1743cm⁻¹ (ester C=O) and 2920cm⁻¹ (C-H stretch), confirming accumulation of triacylglycerols and altered lipid-protein ratios. These patterns are consistent with El-Shenody et al. (2022) and Hounslow et al. (2021), who demonstrated that lipid-associated carbonyl bands intensify with increasing salinity stress, while amide peaks broaden due to protein unfolding. The relative increase in lipid/amide I ratio under high NaCl further substantiates biochemical reallocation toward neutral lipids. Collectively, these results depict a tightly coupled physiological cascade under NaCl stress: Optimal salinity (100 mM) maintains cell turgor, enzyme activity, and pigment stability, maximizing biomass and photosynthetic efficiency. Excess NaCl (≥ 300 mM) disrupts ionic balance, suppressing chlorophyll and growth while stimulating lipid accumulation as a protective energy sink.

Deficiency (0 mM) restricts osmotic balance and chlorophyll biosynthesis, producing suboptimal productivity. This biphasic pattern underscores the feasibility of two-stage cultivation first optimizing biomass under moderate salinity, and then inducing lipid accumulation via controlled salt stress (Ho et al., 2019; Azizi et al., 2021). The consistency between physiological metrics and FTIR-based biochemical markers strengthens the mechanistic understanding of salinity-mediated metabolic remodeling in Chlorella vulgaris. At optimal salinity, homeostasis between chlorophyll synthesis and lipid formation sustains balanced metabolism, leading to higher overall productivity. Beyond the tolerance threshold, oxidative stress dominates, shifting metabolism toward lipid storage at the expense of photosynthesis and cell division. This balance is crucial for biofuel applications, as controlled salinity can be used to strategically induce lipid accumulation without irreversible cellular damage. Similar physiological insights have been applied to two-stage cultivation models where growth and lipid induction phases are temporally separated (Ho *et al.*, 2019; Azizi *et al.*, 2021).

CONCLUSION

The present study comprehensively demonstrates that sodium chloride (NaCl) concentration exerts a dual influence on the growth and metabolism of Chlorella vulgaris. When supplied at optimal levels (around 100 mM), NaCl supports balanced osmotic regulation, pigment integrity, and maximum biomass productivity, indicating its essential physiological role. Both NaCl deficiency and abundance, however, disrupted cellular homeostasis, reduced chlorophyll content, and slowed growth.

At elevated salinity, the alga responded by redirecting carbon flux toward neutral lipid synthesis, resulting in significant enhancement of total lipid content while overall biomass declined. This metabolic shift was further validated by FTIR spectral alterations that reflected increased lipid carbonyl bands and structural changes in cellular proteins, confirming biochemical remodeling under osmotic stress.

The results establish that salinity can be strategically manipulated to achieve a desirable balance between growth and lipid yield. Employing a two-stage cultivation approach-first promoting biomass accumulation under moderate salinity, followed by a stress phase with controlled NaCl elevation-can substantially improve biofuel potential without compromising culture stability.

In conclusion, NaCl acts not merely as a stressor but as a regulator, that governs energy allocation, pigment stability, and metabolic adaptation in Chlorella vulgaris. A deeper understanding of these salinity-driven mechanisms can guide the development of optimized algal production systems for sustainable bioenergy, nutraceutical, and environmental applications.

ACKNOWLEDGEMENT

The authors thank the Head Department of Botany, A.N. College, Patliputra University, Patna, Bihar for providing facilities. Appreciation is also extended to the faculty and staff members for their assistance.

CONFLICT OF INTEREST

The author declares none conflict of interest

REFERENCES

- Arnon, D. I. (1949). Copper enzymes in isolated chloroplasts. *Plant Physiology*, 24(1), 1–15. https://doi.org/10.1104/pp.24.1.1
- Azizi, K., Rahman, S., & Chen, W. (2021). Salinity-dependent modulation of lipid accumulation in *Chlorella vulgaris*. *Algal Research*, 56, 102328. https://doi.org/10.1016/j.algal.20 21.102328
- Bilanovic, D., Andargatchew, A., Kroeger, T., & Shelef, G. (2020). Influence of NaCl concentration on microalgae growth. *Bioresource Technology Reports*, 11, 100497. https://doi.org/10.1016/j.biteb.20 20.100497
- Bligh, E. G., & Dyer, W. J. (1959). A rapid method of total lipid extraction and purification. *Canadian Journal of Biochemistry and Physiology*, 37(8), 911–917. https://doi.org/10.1139/o59-099
- Cheng, P., Ji, B., Gao, L., Zhang, W., & Zhang, C. (2019). Mechanistic insights into salt-induced lipid accumulation in *Chlorella vulgaris*. *Journal of Applied Phycology*, 31(3), 1763–1775. https://doi.org/10.1007/s108 11-019-01775-1
- Chokshi, K., Pancha, I., & Mishra, S. (2022). Enhanced lipid accumulation under NaCl stress in *Chlorella sorokiniana*: A two-stage cultivation approach. *Biotechnology Reports*, 34, e00723. https://doi.org/10.1016/j.btre. 2022.e00723
- Do, J.M., Yeo, H.T., Suh, H.S. and Yoon, H.S., (2023). Effect of salt stress on the biomass productivity and potential bioenergy

- feedstock of *Graesiella emersonii* KNUA204 isolated from Ulleungdo Island, South Korea. *Frontiers in Energy Research*, 11, p.1056835. https://doi.org/10.33 89/fenrg.2023.1056 835 Frontiers
- El-Araby, M., Hassan, M., & El-Shenody, R. (2020). Biochemical and morphological responses of *Chlorella vulgaris* to salinity stress. *Environmental Research*, 188, 109763. https://doi.org/10.1016/j.envres.2020. 109763
- El-Shenody, R. A., Khaled, M. S., & Ashour, M. (2022). FTIR-based characterization of salinity-stressed microalgae: A biochemical fingerprinting approach. *Algal Research*, 66, 102776. https://doi.org/10.1016/j.algal.20 22.102776
- Esteves, A.F., Gonçalves, A.L., Vilar, V.J. and Pires, J.C., 2025. Exploring salinity-induced biochemical changes in *Chlorella vulgaris* using statistical modelling. *Scientific Reports*, 15(1), p.36521. https://doi.org/10.1038/s41598-025-11110-x Nature
- Gao, F., Li, C., & Wang, Y. (2021). Enhanced lipid accumulation and antioxidant activity in *Scenedesmus obliquus* under NaCl stress. *Bioresource Technology*, 339, 125635. https://doi.org/10.1016/j.biortech.20 21.125635
- Gupta, R., & Pawar, R. (2021). Chlorophyll degradation and lipid metabolism under saline stress in green microalgae. *Plant Physiology Reports*, 26(4), 750–759. https://doi.org/10.1007/s40502-021-00590-9
- Ho, S. H., Chen, C. Y., & Chang, J. S. (2019). Effect of salinity on microalgal lipid productivity and biochemical composition: Implications for biofuel applications. *Bioresource Technology*, 289, 121722. https://doi.org/10.1016/j.biortech.2019.121722
- Hounslow, M., Taylor, R., & Baker, A. (2021). FTIR investigation of stress-induced protein alterations and lipid remodeling in *Chlorella vulgaris*. Spectrochimica Acta Part A: Molecular and Biomolecular Spectroscopy,

- 249, 119344. https://doi.org/10.1016/j.saa. 2020.119344
- Huang, X., & Wang, Y. (2022). Enhancing microalgal lipid accumulation for biofuel production: recent advances and future perspectives. *Frontiers in Microbiology*, 13, 1024441. https://doi.org/10.3389/fmicb.2022. 1024441
- Jin, P., Cao, H., & Hu, Q. (2022). Salinity-triggered lipid remodeling in *Nannochloropsis oceanica*: A transcriptomic and metabolomic perspective. *Frontiers in Plant Science*, 13, 835621. https://doi.org/10.3389/fpls.2022. 835621
- Kong, Q., Li, L., & Martinez, R. (2018). Salt-stress enhancement of triacylglycerol in *Chlorella vulgaris*: Role of oxidative signaling and metabolic regulation. *BioEnergy Research*, 11(4), 987–997. https://doi.org/10.1007/s12155-018-9912-5
- El-fayoumy, E. A., Ali, H. E. A., Elsaid, K., Elkhatat, A., Al-Meer, S., Rozaini, M. Z. H., & Abdullah, M. A. (2024). Co-production of high density biomass and high-value compounds via two-stage cultivation of *Chlorella vulgaris* using light intensity and a combination of salt stressors. *Biomass Conversion and Biorefinery*, 14(18), 22673-22686.
- Niu, Y., Yu, X., & Li, F. (2023). Dual role of NaCl in biomass inhibition and lipid induction in *Tetraselmis subcordiformis*. *Algal Research*, 71, 103115. https://doi.org/10.1016/ j.algal.2023.103115

- Paliwal, C., Mitra, M., & Mishra, S. (2020). Salinity-induced lipid enhancement and oxidative stress response in green microalgae: A mechanistic insight. *Frontiers in Microbiology*, 11, 561. https://doi.org/10.3389/fmicb.2020.00561
- Salmeron Covarrubias, L. P., Beluri, K., Mohammadi, Y., Easmin, N., Palacios, O. A., & Sharifan, H. (2025). Advanced Nanoenabled Microalgae Systems: Integrating Oxidative Stress-Induced Metabolic Reprogramming and Enhanced Lipid Biosynthesis for Next-Generation Biofuel Production. ACS Applied Bio Materials, 8(4), 3513-3524.
- Stanier, R. Y., Kunz, H. C., & Cohen-Bazire, G. (1971). Purification and properties of unicellular blue-green algae and their use as reference phototrophs. *Bacteriological Reviews*, 35(2), 171–205.
- Wang, F., Chen, Z., & Liu, Y. (2020). Physiological response and chlorophyll dynamics of *Chlorella vulgaris* under NaCl stress. *Photosynthetica*, 58(1), 231–240. https://doi.org/10.32615/ps.2020.004
- Zhou, JM., Ma, CY., & Liu, LH. (2018). Temporal scaling of the growth dependent radiative properties of microalgae. *arXiv.* (Preprint) arXiv